

Atomic Excitation by Twisted Photons

Andrei Afanasev,¹ Carl E. Carlson,² and Asmita Mukherjee³

¹*Department of Physics, The George Washington University, Washington, DC 20052, USA*

²*Department of Physics, The College of William and Mary in Virginia, Williamsburg, VA 23187, USA*

³*Department of Physics, Indian Institute of Technology Bombay, Powai, Mumbai 400076, India*

(Dated: July 19, 2022)

We show that the twisted photon states, or photon states with large ($> \hbar$) angular momentum projection in the direction of motion, can photoexcite atomic levels having a distribution of quantum numbers in the final state, which are novel and distinct from the excited states produced by plane-wave photons. We considered a general case when the symmetry axis of the twisted-photon beam does not coincide with the center of the atomic target. Numerical calculations are presented using a hydrogen atom as an example. Interesting implications and observables for the above process are pointed out.

The fact that circularly polarized photons carry an angular momentum \hbar was predicted theoretically and demonstrated experimentally in a seminal experiment by Beth in 1936 [1]. It was also realized [2] (Appendix) that the electromagnetic wave can carry orbital angular momentum in the direction of its propagation if it is constrained in the transverse plane, as in the waveguides. Much later, in 1992, Allen and collaborators suggested [3] that a special type of light beams that can propagate in vacuum, called Laguerre-Gaussian, predicted as non-plane wave solutions of Maxwell equations, can carry large angular momentum $J_z \gg \hbar$ associated with their helical wave fronts. At a quantum level such beams can be described in terms of "twisted photons" [4]. This concept can be also extended to beams of particles, and electrons in particular [5]. Detailed reviews of the field are published, *c.f.* [6]. Methods to produce "twisted" light include spiral phase plates, computer-generated holograms [6], synchrotron radiation in a helical undulator [7, 8], or in a free-electron laser [9]. Theoretical work [10, 11] has shown that one can generate twisted photons with high energies of several GeV via Compton back-scattering of laser photons on an energetic electron beam, making such photon beams relevant for nuclear and particle physics.

An important question is, to what extent absorption of the twisted photons by atoms or nuclei is different from the plane-wave photons? Work by Picón *et al.* [12] demonstrated that during photoionization of atoms, the knocked-out electrons carry angular momenta that reproduce the angular momentum of the incoming photons. The reference [12] deals only with a special case in which the photon beam's symmetry axis coincides with a center of an atom. In a recent publication [13] the authors analyzed elastic scattering of the twisted photons on a hydrogen atom, again with a restriction that the atom is located at the center of the optical vortex. We consider a more general case of arbitrary positioned beams and considered photoexcitation of bound states with different quantum numbers in a hydrogen atom.

The twisted photon definition here follows a wave-packet expansion of Serbo and Jentschura [10, 11]. An-

other possibility would be to quantize a Laguerre-Gaussian laser mode considered in the original work by Allen *et al.* [3]. We treat the atom nonrelativistically so the interaction Hamiltonian is $H_1 = -(e/m_e)\vec{A} \cdot \vec{p}$.

We place the atomic nucleus at the origin, with the atomic electron located at (ρ, ϕ_ρ, z) in cylindrical coordinates or (r, θ_r, ϕ_ρ) in spherical coordinates. The twisted photon, moving in the z -direction, has its origin in general not centered on the atomic nucleus but displaced to position \vec{b} in the x - y plane. Relative to the photon axis, the electron position projected onto the x - y plane will be at a distance $|\vec{p} - \vec{b}|$ and angle ϕ'_ρ , as illustrated in Fig. 1.

The 4-vector potential A^μ of the twisted photons with helicity Λ , momentum and total angular momentum projection on z -axis respectively k_z and m_γ , is given by

$$\begin{aligned} A_{km_\gamma k_z \Lambda}^\mu(x) = & e^{-i(\omega t - k_z z)} \left\{ \frac{\Lambda}{\sqrt{2}} e^{im_\gamma \phi_\rho} \sin \theta_k J_{m_\gamma}(\kappa \rho) \eta_0^\mu \right. \\ & + i^{-\Lambda} e^{i(m_\gamma - \Lambda) \phi_\rho} \cos^2 \frac{\theta_k}{2} J_{m_\gamma - \Lambda}(\kappa \rho) \eta_\Lambda^\mu \\ & \left. + i^\Lambda e^{i(m_\gamma + \Lambda) \phi_\rho} \sin^2 \frac{\theta_k}{2} J_{m_\gamma + \Lambda}(\kappa \rho) \eta_{-\Lambda}^\mu \right\} \sqrt{\frac{\kappa}{2\pi}}. \end{aligned} \quad (1)$$

where κ is the transverse momentum and the η 's are constant vectors,

$$\eta_{\pm 1}^\mu = \frac{1}{\sqrt{2}} (0, \mp 1, -i, 0), \quad \eta_0^\mu = (0, 0, 0, 1); \quad (2)$$

Using the above expression for the vector potential and the expansion of complex exponential in terms of Bessel functions, we obtain the matrix element for transitions from the ground to excited states of the hydrogen atom. An atomic state is defined in terms of its principal quantum number n_k , orbital quantum number l_k , and magnetic quantum number m_k , where $k = i$ for the initial state and $k = f$ for the final state. The matrix element is

$$\begin{aligned}
S_{fi} &= -2\pi\delta(E_f - E_i - \omega) \frac{e}{m_e a_0} \sqrt{\frac{2\pi\kappa}{3}} e^{i(m_\gamma - m_f)\phi_b} J_{m_f - m_\gamma}(\kappa b) \\
&\times i^{-\Lambda} \left\{ \cos^2 \frac{\theta_k}{2} g_{n_f l_f m_f \Lambda} + \frac{i}{\sqrt{2}} \sin \theta_k g_{n_f l_f m_f 0} - \sin^2 \frac{\theta_k}{2} g_{n_f l_f m_f -\Lambda} \right\} \\
&\stackrel{\text{def}}{=} 2\pi\delta(E_f - E_i - \omega) \mathcal{M}_{n_f l_f m_f \Lambda}^{(m_\gamma)}(b).
\end{aligned} \tag{3}$$

The dimensionless atomic factors are ($\Lambda' = \pm 1, 0$)

$$g_{n_f l_f m_f \Lambda'} \equiv -a_0 \int_0^\infty r^2 dr R_{n_f l_f}(r) R'_{10}(r) \int_{-1}^1 d(\cos \theta_r) J_{m_f - \Lambda'}(\kappa \rho) Y_{l_f m_f}(\theta_r, 0) Y_{1\Lambda'}(\theta_r, 0) e^{ik_z z}, \tag{4}$$

and a_0 is the Bohr radius. The quantum numbers of the initial state are tacit. One can show that the three terms in the curly bracket above are either all real or else all purely imaginary.

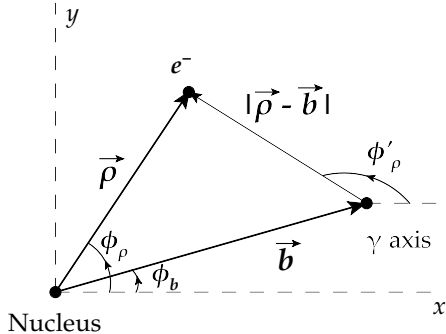


FIG. 1: Relative positions of atomic state and photon axis, as projected onto the x - y plane, with the origin at the nucleus of the atom.

By way of review, the selection rules for photoexcitation (starting from the ground state) with plane wave photons of helicity Λ are, *cf.* Refs. [14],

$$\begin{aligned}
m_f &= \Lambda, \quad l_f \geq 1, \\
g_{n_f l_f m_f = \Lambda, \Lambda}^{(\text{pw})} &\propto (\omega a_0)^{l_f - 1},
\end{aligned} \tag{5}$$

where $g^{(\text{pw})}$ is the plane wave analog of the reduced atomic amplitudes shown in Eq. (4), and shows the suppression that follows when higher photon partial waves are needed.

For a twisted photon, the magnitude of the result depends on m_γ only through the argument of the Bessel function $J_{m_f - m_\gamma}(\kappa b)$. When a twisted photon strikes an atom centered on its axis, the impact parameter $b = 0$ and we immediately obtain $m_f = m_\gamma$ from the Bessel function in the general result, Eq. (3),

$$J_{m_f - m_\gamma}(\kappa b) \rightarrow J_{m_f - m_\gamma}(0) = \delta_{m_f m_\gamma}. \tag{6}$$

That is, the only final states that can be produced are those that can absorb the full projected orbital angular momentum of the twisted photon.

However, the atom does not have to be far off the photon axis before other amplitudes, not satisfying the above selection rule, play an important role. As illustration, we plot in Fig. 2 the amplitudes $|\mathcal{M}_{n_f l_f m_f \Lambda}(b)|$ for the example of $n_f = 4, l_f = 1, \Lambda = 1$, photon energy and wavelength set by the H-atom level spacing, and photon angular momentum along the direction of motion $m_\gamma = 3$ (upper plot) and $n_f = 4, l_f = 3, \Lambda = 1$ (lower plot). Note the relative strength of the amplitudes is much higher, by about six orders of magnitudes, for the transition into $l_f = 1$ state vs $l_f = 3$, in accordance with the selection rules presented below.

In Fig. 2 the horizontal axis is the impact parameter b in units of the photon wavelength λ . Already with an impact parameter of less than half a wavelength, amplitudes that do not satisfy the $m_f = m_\gamma$ selection rule are becoming important. The amplitude with the largest peak is the one with $m_f = 1$, which is the only amplitude one would have with a plane-wave photon polarized with helicity $\Lambda = 1$. In a near-field setup, if the twisted light outside of the central (small- b) areas is blocked by a screen, one can study whether the enhancement of the transition to $m_f = m_\gamma$ for the photons with large m_γ , as seen in Fig. 2, would lead to enhanced attenuation of these photons by atoms, making matter more opaque to them.

The general selection rules for the off-axis case are

$$\begin{aligned}
m_f &= \text{any}, \quad l_f \geq |m_f|, \\
g_{n_f l_f m_f, \Lambda} &\propto (\omega a_0 \cos \theta_k)^{l_f - |m_f - \Lambda| - 1} (\omega a_0 \sin \theta_k)^{|m_f - \Lambda|},
\end{aligned} \tag{7}$$

where in the last line, the first factor is absent if its exponent is negative.

Note that we neglect atomic recoil. For manifest conservation of both linear and angular momentum, the re-

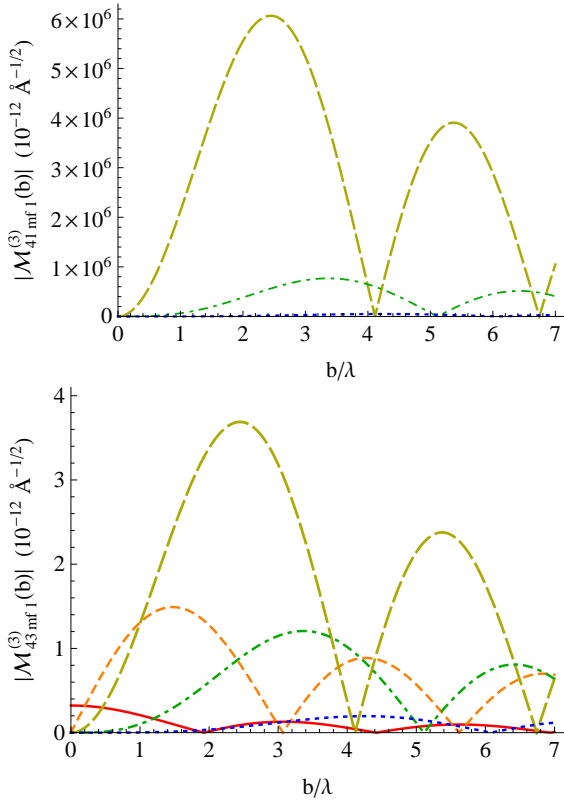


FIG. 2: Size of the transition amplitude $|\mathcal{M}_{n_f l_f m_f \Lambda}^{(m_\gamma=3)}(b)|$ for particular quantum numbers n_f, l_f, Λ and several m_f ; here the photons are circularly polarized with $\Lambda = 1$ and $\theta_k = 0.2$ rad. Upper graph is for the final state $n_f = 4, l_f = 1$; the state $m_f = 1$ is allowed by electric-dipole selection rules for plane waves, while $m_f = 0, -1$ are unique for the twisted photons. Lower graph is for the final state $n_f = 4, l_f = 3$. The curve styles for both graphs are: $m_f = 3$ is the red solid curve, $m_f = 2$ is orange and medium dashed, $m_f = 1$ is gold and long dashed, $m_f = 0$ is green and dot-dashed, $m_f = -1$ is blue and dotted, and transitions to other m_f are quite small and not plotted.

coil momentum of the atom can be taken into account.

In general, if the location of the photon axis cannot be controlled at the level of the atomic spacing, we should average over the transverse separations. For transverse separation \vec{b} within a circular target of radius R ,

$$\sigma_{n_f l_f m_f \Lambda}^{(m_\gamma)} = 2\pi\delta(E_f - E_i - \omega_\gamma) \frac{|\mathcal{M}_{n_f l_f m_f \Lambda}^{(m_\gamma)}(b)|^2}{f}. \quad (8)$$

where f is the incoming flux and a suitable sum or average over spins is implied. However, averaging over the

atom location b , we obtain

$$\bar{\sigma}_{n_f l_f m_f \Lambda} = 2\pi\delta(E_f - E_i - \omega) \frac{8\pi^3\alpha^3}{3k_z} \left| \cos^2 \frac{\theta_k}{2} g_{n_f l_f m_f \Lambda} \right. \\ \left. + \frac{i}{\sqrt{2}} \sin \theta_k g_{n_f l_f m_f 0} - \sin^2 \frac{\theta_k}{2} g_{n_f l_f m_f, -\Lambda} \right|^2. \quad (9)$$

For the twisted photon centered on target, there is the dramatic result that the magnetic quantum number of the final atomic state must equal the corresponding z -projection of orbital angular momentum of the twisted photon. This constraint is relaxed for the general case of random target location, but there are still features unique to twisted photons.

Photoexcitation, starting from the ground state, by a plane-wave photon of a certain helicity leads only to final states whose magnetic quantum number equals the helicity. Twisted photons, on the other hand, photoexcite states with a large range of magnetic quantum numbers m_f . Values of m_f impossible for plane-wave photons are produced even when the twisted photons enter a medium with random target locations.

Twisted photons also produce the $m_f = \Lambda$ states that plane-wave photons necessarily lead to. But the interest is in the $m_f \neq \Lambda$ states unique to twisted photon production. To quantify the probability of finding these states, we define a ratio for a fixed Λ which compares the rate for producing final states that are unique to twisted photons to the total rate where the twisted photon produces all final states, including $m_f = \Lambda$, for a given energy level characterized by quantum numbers (n_f, l_f) (and for the case of a large interaction region with random target locations),

$$f_{\text{twisted}} = \frac{\sum_{\substack{m_f = l_f \\ m_f = -l_f \\ m_f \neq \Lambda}} \bar{\sigma}_{n_f l_f m_f \Lambda}}{\sum_{m_f = -l_f} \bar{\sigma}_{n_f l_f m_f \Lambda}}. \quad (10)$$

The “twisted photon ratio,” f_{twisted} , evaluates what fraction of the final states excited by the twisted photon could not have been produced by a plane-wave photon. As a numerical example, we evaluate this ratio for final states with varied values of n_f and l_f and for a twisted photon with pitch angle of $\theta_k = 0.2$ radians. The energy is fixed by the H-atom level spacing, corresponding to the photon wavelength of 100nm, and the result is

$$f_{\text{twisted}} \left[\text{gnd. state} \rightarrow (n_f = 4, l_f = 1) \right] = 2.0\%, \\ f_{\text{twisted}} \left[\text{gnd. state} \rightarrow (n_f = 4, l_f = 3) \right] = 20.3\%. \quad (11)$$

A comparison between the total photoproduction rate

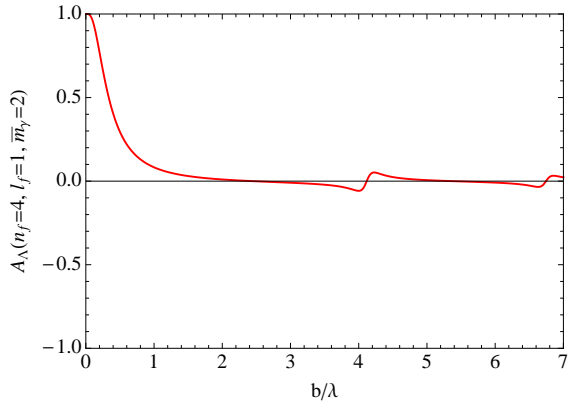


FIG. 3: Helicity asymmetry A_Λ for excitation of the atomic state $n_f = 4, l_f = 1$ by a twisted photon with $\bar{m}_\gamma = 2$.

from twisted photons and from plane-wave photons is,

$$r_{\text{twisted}} = \frac{\sum_{m_f=-l_f}^{m_f=l_f} \bar{\sigma}_{n_f l_f m_f \Lambda}}{\sigma_{n_f l_f \Lambda \Lambda}^{(pw)}}. \quad (12)$$

For the above-chosen final states the other ratio works out to $r_{\text{twisted}} = 1.02$.

The ratios f_{twisted} and r_{twisted} can be measured in experiments. They can provide a tool to identify twisted photons arriving from point-like sources, no matter if they come from distant stars or produced in the lab. In particular, presence of $m_f = 0$ state in the atomic excitation produced by the photons coming from a well-defined direction would be a definitive signal of a twisted photon absorption.

Let us discuss one more special feature of the twisted photons and compare the probabilities of photoexcitation of an (unpolarized) atom by the photons with opposite helicities $\pm \Lambda$. For plane-wave photons these probabilities are identical due to parity conservation. For twisted photons with a fixed z -projection of orbital angular momentum but opposite helicities such an asymmetry would not violate parity, because the corresponding photon states do not transform into each other via parity transformation. The corresponding helicity asymmetry A_Λ can be defined as

$$A_\Lambda(n_f, l_f, \bar{m}_\gamma) = \frac{\sum_{m_f=-l_f}^{m_f=l_f} (\sigma_{n_f l_f m_f \Lambda=-1}^{(\bar{m}_\gamma-1)} - \sigma_{n_f l_f m_f \Lambda=1}^{(\bar{m}_\gamma+1)})}{\sum_{m_f=-l_f}^{m_f=l_f} (\sigma_{n_f l_f m_f \Lambda=-1}^{(\bar{m}_\gamma-1)} + \sigma_{n_f l_f m_f \Lambda=1}^{(\bar{m}_\gamma+1)})} \quad (13)$$

The value of \bar{m}_γ is zero for plane-wave photons; for the twisted photons it is controlled by the method of their generation, and in paraxial approximation it would cor-

respond to z -projection of the orbital angular momentum. The asymmetry A_Λ turns to zero after averaging up to infinite values of the impact parameter b ; it is large for the central areas of the optical vortex, as shown in Fig. 3. This interesting observable can be studied experimentally for micro-particles placed in the inner area of the optical vortex; it indicates that the electromagnetic fields due to spin and orbital angular momentum of the twisted photons add up coherently, leading to distinctively different strength of interaction at a given transverse-plane location if the direction of spin is flipped. The corresponding figure-of-merit $A_\Lambda^2 \sigma$, is small at $b=0$, but peaks near $b/\lambda=0.6$, where A_Λ is about 20%.

In summary, we present results of the calculations for the amplitudes and observables associated with excitation of a hydrogen atom by the twisted photons. We derive new selection rules and predict several unique features of twisted-photon absorption by atoms that can be verified experimentally.

CEC thanks the National Science Foundation for support under Grants PHY-0855618 and PHY-1205905. Work of AA was supported by The George Washington University. AM thanks JLab and College of William and Mary for hospitality and support during initial stages of this work.

- [1] R. Beth, Phys. Rev. **50**, 115 (1936).
- [2] W. Heitler, *The Quantum Theory of Radiation* (Oxford, 1954).
- [3] L. Allen, M. Beijersbergen, R. Spreeuw, and J. Woerdman, Phys. Rev. **A45**, 8185 (1992).
- [4] G. Molina-Terriza, J. P. Torres, and L. Torner, Nature Physics **3**, 305 (2007).
- [5] M. Uchida and A. Tomomura, Nature **464**, 737 (2010).
- [6] A. Yao and M. Padgett, Advances in Optics and Photonics **3**, 161 (2011).
- [7] S. Sasaki and I. McNulty, Phys. Rev. Lett. **100**, 124801 (2008).
- [8] A. Afanasev and A. Mikhailichenko (2011), 1109.1603.
- [9] A. Hemsing, A. Marinelli, and J. Rosenzweig, Phys. Rev. Lett. **106**, 164803 (2011).
- [10] U. Jentschura and V. Serbo, Phys. Rev. Lett. **103**, 013001 (2011), 1008.4788.
- [11] U. Jentschura and V. Serbo, Eur. Phys. J. **C71**, 1571 (2011), 1101.1206.
- [12] A. Picón, J. Mompart, J. R. V. de Aldana, L. Plaja, G. F. Calvo, and L. Roso, Optics Express **18**, 3660 (2010), 1002.1318.
- [13] B. Davis, L. Kaplan, and J. McGuire, Journal of Optics **15**, 035403 (2013), 1206.6935.
- [14] L. Schiff, *Quantum Mechanics* (McGraw-Hill, 1968).